

CAVITATION EROSION OF Ti-6Al-4V ALLOY WITH VACUUM-ARC TiN AND CrN COATINGS

*A.S. Kuprin¹, V.D. Ovcharenko¹, S.A. Leonov¹, G.N. Tolmachova¹, V.A. Belous¹,
E.N. Reshetnyak¹, I.O. Klimenko¹, M. Kmech²*

¹*National Science Center “Kharkov Institute of Physics and Technology”,
Kharkov, Ukraine;*

²*Gdansk Polytechnic University, Gdansk, Poland*

E-mail: kuprin@kipt.kharkov.ua

The distilled-water cavitation erosion resistance of Ti-6Al-4V alloy with vacuum-arc TiN and CrN coatings is investigated. The results show that the coatings having high mechanical properties are capable to reduce appreciably the cavitation erosion of the alloy by prolonging the incubation period of fracture and by decreasing the mass loss. Preliminary ion-plasma nitriding of the alloy leads to the formation under the coating of a solid transition layer which enhances the coating alloy adhesion and so increases the alloy resistance to the cavitation erosion.

INTRODUCTION

Titanium alloys, possessing a high strength-to-weight ratio and good high-temperature and corrosion resistance, are widely applied in aerospace, atomic, defense industries and medicine. This material is promising for turbine blades, however, under cavitation erosion conditions, particularly, in corrosive media, the intense blade surface erosion occurs that decreases the turbine service life. It is well-known [1] that the cavitation erosion decreases with material hardness increasing. The cavitation erosion resistance of titanium and its alloys in the corrosive medium was investigated in [2, 3]. It is shown that by increasing the hardness of titanium alloys the cavitation wear can be reduced that improves their corrosion properties. One of the means for titanium alloy protection is to deposit hard and corrosion-resistant coatings on the base of nitrides, carbides etc.

Methods of steels and titanium alloy protection against cavitation are extensively studied [4–12]. Formation with a laser of a hard nitride layer having a dendritic structure on titanium and Ti-6Al-4V alloys substantially decreases their cavitation erosion [4]. A laser-formed TiC coating increases in 1.2...1.8 times the cavitation erosion resistance of Ti-6Al-4V alloy [5]. The cavitation erosion resistance of steels has been significantly increased by the vacuum-arc deposition of TiN, CrN, and multilayer Ti/TiN coatings with different combinations of the layer number and thickness [6–8]. These papers note that the specimens with coatings of 4...8 μm thickness demonstrate the best cavitation resistance. The subsequent coating thickness decrease reduces a positive cavitation resistance effect as the adhesion between the thick strained coating layer and the substrate becomes worse. The results of paper [9] show that the TiN coating increases the cavitation erosion resistance of Ti-6Al-4V alloy in 4...8 times depending on the conditions of their formations. The vacuum-arc coatings increase considerably the abrasion wear resistance of gas turbine blades [10]. Plasma carburizing of Ti-6Al-4V surface with subsequent CrN coating deposition has enhanced by 30...40% the fatigue resistance and by 60% the wear resistance of the alloy

[11]. Nitriding of the Ti-6Al-4V surface before CrN coating deposition improves the tribologic properties and decreases the wear rate of the alloy due to the formation of a hard layer containing TiN and Ti₂N under the coating [12].

The purpose of this study is to investigate the effect of vacuum-arc TiN and CrN coating deposition and preliminary nitriding on the Ti-6Al-4V cavitation erosion resistance.

1. EXPERIMENTAL TECHNIQUE

Coatings were deposited on the end surface of Ti-6Al-4V specimens by the vacuum-arc method on the installation “Bulat-6”. An evaporator with magnetic stabilization of a cathode spot was applied [13]. Cathode materials were Cr (99.9%) and Ti (99.9%). Initial vacuum in the chamber was at a level of 1·10⁻³ Pa. Before coating deposition the specimen surface was subjected to the sputtering by cathode material ions at a negative bias voltage of 1.2 kV. The temperature of specimens did not exceed 450 °C. The vacuum arc current in the process of deposition was 100 A, nitrogen pressure was in the range of 1.5...2 Pa. The distance between the cathode and planet-rotating specimens was 250 mm. In the process of deposition a negative bias voltage of 300 V was applied to the samples. Before the coating deposition a part of samples was subjected to the ion-plasma nitriding at temperatures of 700 °C for 30 min under nitrogen pressure of ~ 0.7 Pa.

The adhesion of the deposited coating was evaluated by the method of Rockwell-C adhesion tests under the load of 150 kg [14]. Mechanical properties of the coatings were investigated by the nanoindentation methods using a device Nanoindenter G200 with a CSM [15]. The phase composition of specimens in the initial state and after coating deposition was investigated by the X-ray diffraction analysis using a diffractometer DRON-3 in the filtered radiation of a copper anode.

Diffraction patterns were recorded in the θ-2θ scanning with Bragg-Brentano focusing in the range of angles from 20 to 80 degrees. By the position of diffraction lines we determined the periods of the crystalline lattice of identified phases in the direction of

the normal to the film direction. The coherent scattering region (CSR) size was determined by the line broadening using the Sherrer relation.

Cavitation tests were carried out in distilled water using a Hielsher-UP400St device presented in Fig.1 at temperature of 70 °C when the cavitation wear in water is maximal [1, 3]. The distance from the emitter to the specimen was 0.5 mm, the oscillation amplitude was 50% at a frequency of 23.76 kHz and a power of 100 W.

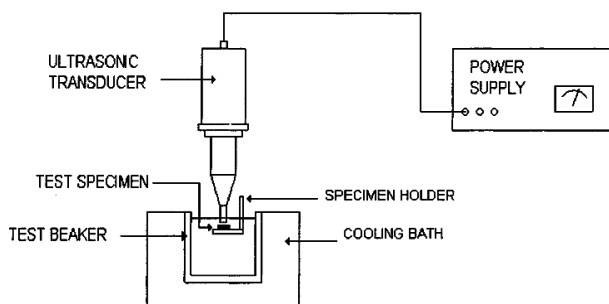


Fig. 1. Test device Hielsher-UP400St

2. RESULTS AND DISCUSSION

Fig. 2 shows the photos of the samples with coatings. The TiN and CrN coatings having golden and grey color, formed by the vacuum-arc technique, possess high mechanical properties.



Fig. 2. Photos of Ti-6Al-4V samples without coatings and with vacuum-arc coatings

In Table given are the thickness, hardness and Young modulus of the coatings and the adhesion values obtained by the Rockwell-C adhesion tests.

As it follows from the table, the hardness values of TiN, CrN coatings are 30 and 20, and the Young modulus values are 400 and 350 GPa, respectively. The best coating-alloy adhesion is in the case of preliminary surface nitriding of the alloy and corresponds, by the Rockwell-C adhesion tests, to the HF1 value, while without surface modification it is HF2. In this case one can see small cracks in the corresponding images.

The worst of all is the adhesion to the alloy of the CrN coating of a 10 μm thickness. Under the load of 150 kg the hard ($H = 20$ GPa) and thick coatings, deposited on the Ti-6Al-4V alloy ($H = 4$ GPa) are cracking.

Fig. 3 presents the diffraction patterns of the investigated specimens. The diffraction pattern of the Ti-6Al-4V specimen in the initial state (see Fig. 3,a) shows the lines of two polymorphous titanium modifications, α -Ti and β -Ti depending on the Ti alloy composition. The α -Ti phase has a face-centered close-packed (fcc) lattice with parameters: $a = 0.295$ nm, $c = 0.469$ nm ($c/a = 1.59$). The high-temperature β -Ti modification has a bcc lattice with period $a = 0.329$ nm.

Thickness (h), hardness (H), Young modulus (E) and coating adhesion (HF) on the Ti-6Al-4V alloy

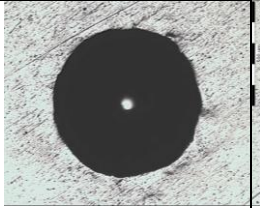
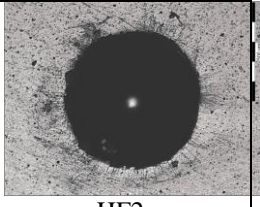
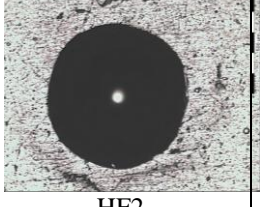

Coating	h , μm	H , GPa	E , GPa	Adhesion
CrN	4	20	350	 HF2
CrN	10	20	350	 HF2
TiN	4	30	400	 HF2
TiN+N ₂	15	30	400	 HF1

Fig. 3,b presents the diffraction pattern of the Ti-6Al-4V sample with the TiN coating deposited on its surface. A single substrate line clearly visible in the diffraction pattern is (101) α -Ti. It is the strongest line in the diffraction pattern of the initial Ti-6Al-4V alloy.

Apart from the faint substrate line there are visible in the diffraction pattern two very strong rather narrow lines of the coating: reflections (111) and (222) of the cubic TiN nitride (structural type of NaCl). Other lines of this phase are absent that is explained by the formation in the coating of a strong axial-type texture with axis [111] with the normal directed to the surface.

The lattice constant of TiN is 0.426 nm that is slightly higher than the table value for this phase ($a_{\text{TiN}} = 0.424$ nm) and caused by the formation of compression residual stresses in the coating. The crystallite size of nitride is 40 nm.

The diffraction pattern of the Ti-6Al-4V alloy after nitriding and subsequent deposition of the TiN coating is presented in Fig. 3,c. Substrate lines in the diffraction pattern are not visible.

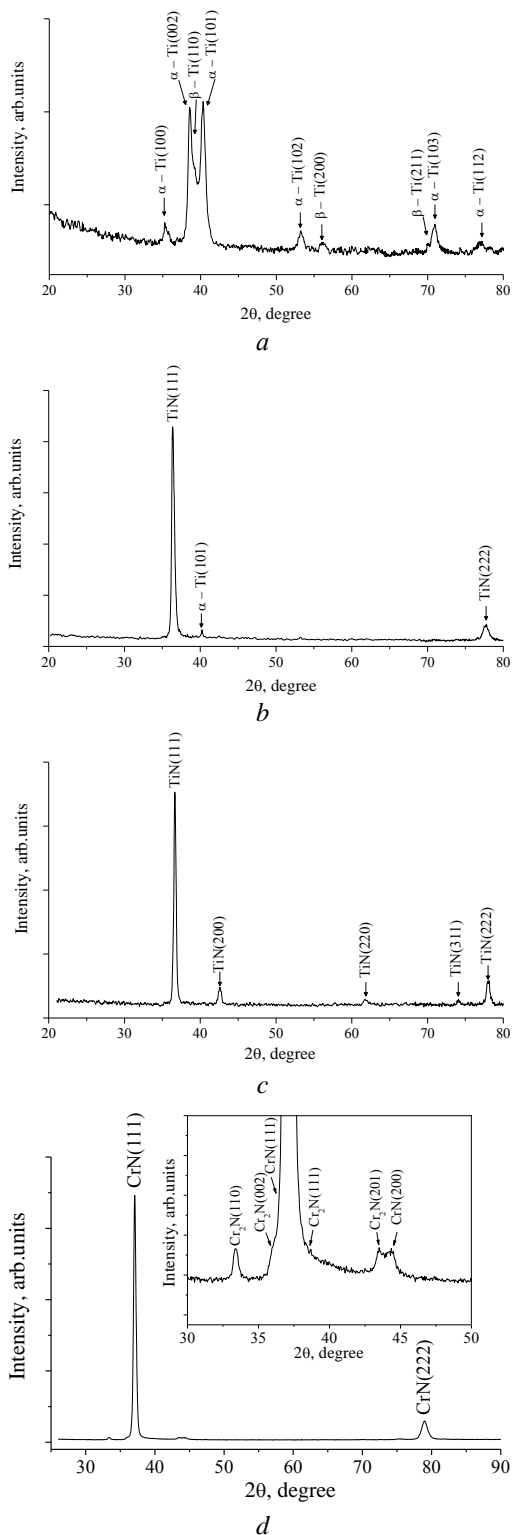


Fig. 3. Diffraction patterns of Ti-6Al-4V specimens: a – initial alloy; b – with TiN coating; c – after nitriding with TiN coating; d – with CrN coating

Narrow strong lines (111) and (222) of TiN in Fig. 3,c belong to the textured coating. The lattice constant of TiN in the coating is 0.425 nm. This value is lower than that in the coating deposited onto the substrate without nitriding that, most likely, is related with residual stress level decreasing. The nitride crystallite size in the coating is 60 nm. In the diffraction

pattern (see Fig. 3,c) faint reflections of TiN with indices (200), (220), and (311) take place too. They correspond to nitride with the lattice spacing of 0.424 nm and crystallite size of about 30 nm, which has been apparently formed in the nitride layer.

In Fig. 3 given is the diffraction pattern of the Ti-6Al-4V specimen with the CrN coating deposited on its surface. In the coating simultaneously exist two nitride phases: cubic CrN (structural type of NaCl) and a little amount of hexagonal Cr₂N, formed due to the nitride deficiency. Diffraction lines (111) and (222) of CrN are much stronger than the rest reflections. The crystalline lattice parameter of CrN in the coating is $a = 0.419$ nm, that is higher than the table value of this phase ($a_{CrN} = 0.416$ nm). So, in this phase, similarly to that in TiN, a strong axial texture with axis [111] and compression stresses are presented. The CrN-phase crystallite size is 36 nm.

The hardness distribution in the depth, measured on the transverse sections taken from the initial alloy and alloy with TiN coatings of 4 and 15 μm , after nitriding and without nitriding its surface, is shown in Fig. 4. The Ti-6Al-4V alloy hardness is 4 GPa and is not changing in the depth. In the alloy after nitriding a thicker layer is formed. Its hardness decreases from 12 GPa at the depth of 15 μm to the initial one of 4 GPa at a distance of 40 μm from the surface. The transition layer length depends essentially on the layer surface temperature which, in our case is determined by the voltage on the substrate, nitriding time, as well as, by the pressure of nitrogen and substrate condition.

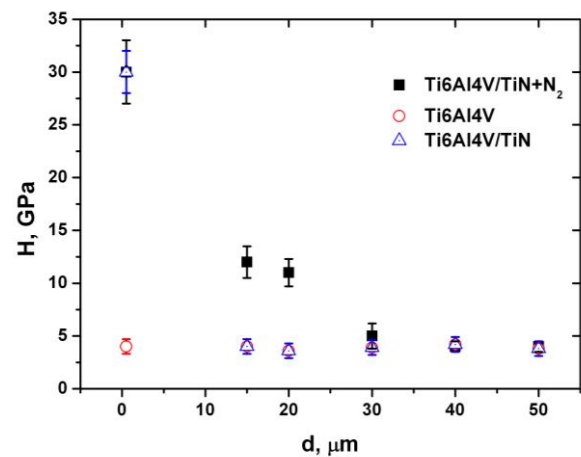


Fig. 4. Hardness distribution in the depth of the three Ti-6Al-4V samples: initial, with TiN coating and after nitriding with TiN coating

For comparison the microstructure formed in the different samples is shown by the photos in Fig. 5. Fig. 5,a presents the section from the specimen with the TiN coating of 4.2 μm thickness. One can clearly see the coating of a corresponding thickness and the fine-grained structure of Ti-6Al-4V alloy which increases the alloy hardness [16].

On the section from the specimen with the TiN coating of 15 μm (see Fig. 5,b), deposited after preliminary alloy nitriding, one can observe (1) the presence of transition layer (2) and diffusion zone (3) under the coating. Nitriding of the Ti-6Al-4V alloy

leads to the synthesis of titanium nitrides, having different stoichiometric composition (TiN, Ti₂N), and to the formation of a subsurface transition layer, having a fine-grained equiaxial structure [17]. This is explained by the alloy structure and nitriding temperature at which different diffusion processes occur [17].

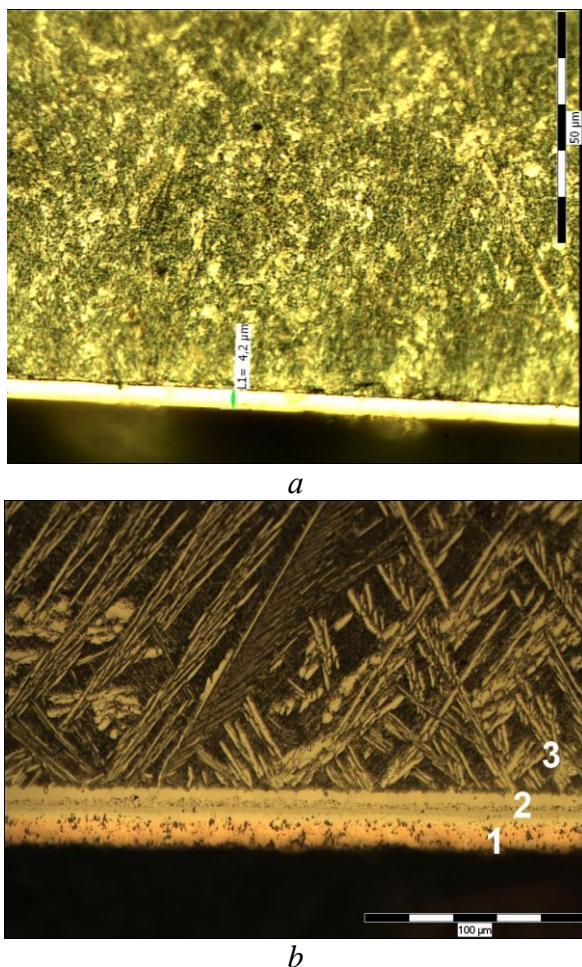


Fig. 5. Optical microscopy of Ti-6Al-4V alloy section with TiN coating: a – without nitriding (x100), b – with nitriding (x50)

The total thickness of the coating and transition layer after nitriding is ~ 35 μm that corresponds to Fig. 4.

The diffusion zone has an equiaxial and acicular basket structure. The elongated parts in the form of plates present the α-phase and there are mixtures of α- and β-phases and nitrogen-based solid solution between these parts [17]. The diffusion zone, which reaches the depth of 195 μm, is smoothly changing into the fine-grained alloy structure.

So, as a result of the preliminary alloy nitriding a transition harder layer is formed under the coating that can exert influence on the cavitation resistance of specimens with the coating.

Fig. 6 presents the photos of the Ti-6Al-4V alloy samples with the TiN and CrN coatings of different thicknesses after the cavitation erosion during the indicated time.

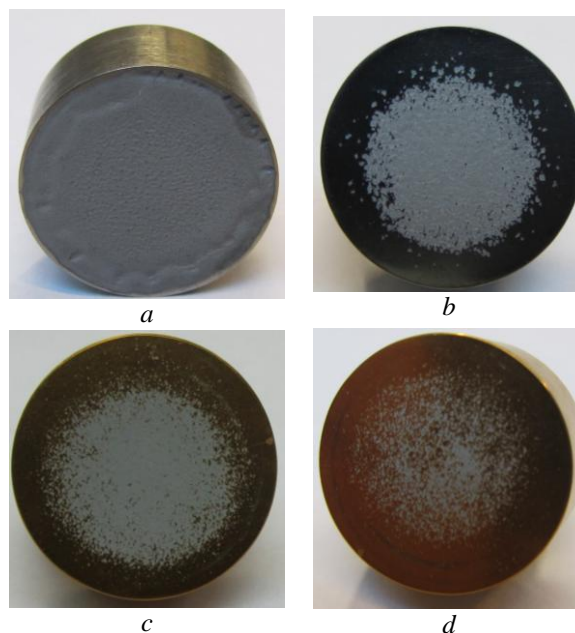


Fig. 6. Photos of samples after the cavitation erosion: a – Ti-6Al-4V alloy, 350 min; b – with CrN coating (4 μm, 600 min); c – with TiN coating (4 μm, 550 min); d – with TiN coating and nitriding (15 μm, 700 min)

It is clearly seen that the coatings shown in Fig. 6, b,c,d significantly decrease the cavitation erosion of Ti-6Al-4V alloy.

The samples mass loss with cavitation time is presented in Fig. 7. The nitride TiN and CrN coating having the thickness of 3...4 μm prolongs the incubation period before fracture by 3...4 h and decrease the samples mass loss in seven times during the same test time as compared to Ti-6Al-4V alloy.

The CrN coating of 10 μm thickness deposited on the soft alloy surface does not change the sample mass loss in comparison with the uncoated alloy. Preliminary nitriding for 10 h and TiN coating formation do not deteriorate at all the sample and then its mass loss rate coincides with that of Ti-6Al-4V alloy.

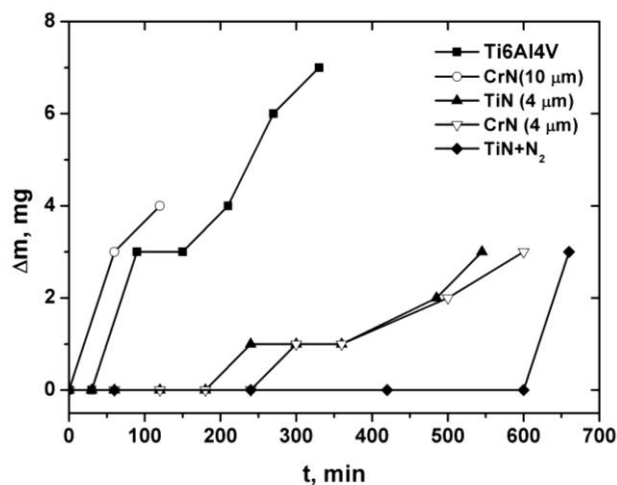


Fig. 7. Cavitation erosion of Ti-6Al-4V alloy with ion-plasma coatings

A high cavitation erosion resistance of the samples is explained by a higher thickness (15 μm) of the nitride coating and a higher adhesion (HF1) to the hard nitrided layer of the alloy. The specimen with a thick CrN coating is deteriorates similarly to Ti-6Al-4V alloy. As it follows from [7, 8, 19] only a little increase of the thickness of the coatings deposited on the nonhardened steel surface reduces the cavitation erosion resistance. It can be explained by the lower adhesion of the thick stresses nitride coating to the substrate.

CONCLUSION

The vacuum-arc method has been used for deposition on the Ti-6Al-4V alloy surface the TiN and CrN coatings having a cubic structure and a strong equiaxial structure [111] with high mechanical properties: $H = 30$ and 20 GPa, $E = 400$ and 350 GPa, respectively.

The coatings of 3...4 μm thickness increases the Ti-6Al-4V alloy cavitation erosion resistance by prolonging the incubation period before fracture in 6...8 times and decreasing the cavitation erosion rate in 7 times. The coating of 10 μm does not possess protective properties because of a low adhesion. Preliminary alloy nitriding results in formation under the coating of a hard transition titanium nitride layer that leads to the adhesion enhancement.

The TiN coating of 15 μm thickness deposited on the nitrided Ti-6Al-4V alloy surface provides the best cavitation erosion resistance.

REFERENCES

1. I. Pirson. *Kavitation*. M.: "Mir", 1975, p. 95.
2. A. Neville, B.A.B. McDougall. Erosion- and cavitation-corrosion of titanium and its alloys // *Wear*. 2001, v. 250, p. 726-735.
3. H. Mochizuki, M. Yokota, S. Hattori. Effects of materials and solution temperatures on cavitation erosion of pure titanium and titanium alloy in seawater // *Wear*. 2007, v. 262, p. 522-528.
4. H.C. Man, Z.D. Cui, T.M. Yue, F.T. Cheng. Cavitation erosion behavior of laser gas nitrided Ti and Ti6Al4V alloy // *Materials Science and Engineering A*. 2003, v. 355, p. 167-173.
5. M. Duraiselvam, R. Galun, V. Wesling, B.L. Mordike, R. Reiter, J. Oligmüller, G. Buvanashakaran. Cavitation erosion resistance of Ti6Al4V laser alloyed with TiC-reinforced dual phase intermetallic matrix composites // *Materials Science and Engineering A*. 2007, v. 454-455, p. 63-68.
6. A. Krella. The experimental resistance parameter for TiN coating to cavitation action // *Advances in Materials Science*. 2010, v. 10, N 1(23), p. 4-18.
7. A. Krella. Cavitation erosion of TiN and CrN coatings deposited on different substrates // *Wear*. 2013, v. 297, p. 992-997.
8. A. Krella. Cavitation erosion resistance of Ti/TiN multilayer coatings // *Surface and Coatings Technology*. 2013, v. 228, p. 115-123.
9. V.A. Belous, V.N. Voeyvodin, V.M. Khoroshikh, G.I. Nosov, V.G. Marinin, S.A. Leonov, V.D. Ovcharenko, V.I. Kovalenko, A.A. Komar, A.S. Kuprin, L.O. Shpagina. Prototype equipment and techniques for obtaining cavitation-resistant coatings to be applied to working surfaces of steam turbine blades made of VT6 titanium alloy in order to replace imported counterparts // *Sci. Innov.* 2016, v. 12(4), p. 27-35.
10. V.A. Belous, V.V. Vasilyev, S.K. Goltvyanitsa, V.S. Goltvyanitsa, Yu.A. Zadneprovsky, V.I. Kovalenko, A.S. Kuprin, N.S. Lomino, A.A. Luchaninov, V.G. Marinin, V.D. Ovcharenko, E.N. Reshetnyak, V.E. Strelnitsky, G.N. Tolmachova. Abrasive and cavitation erosion resistance of TiN coatings, alloyed with Al, Si, Y // *Visnyk dvygunobuduvannya*. 2012, N 1, p. 201-205 (in Ukrainian).
11. Y.G. Park, M.Y. Wey, S.I. Hong. Enhanced wear and fatigue properties of Ti-6Al-4V alloy modified by plasma carburizing/CrN coating // *J Mater Sci: Mater Med*. 2007, v. 18, p. 925-931.
12. J. Jin, H. Duan, X. Li. The influence of plasma nitriding on microstructure and properties of CrN and CrNiN coatings on Ti6Al4V by magnetron sputtering // *Vacuum*. 2017, v. 136, p. 112-120.
13. I.I. Aksenov, A.A. Andreev, V.A. Belous, V.E. Strel'nitskij, V.M. Khoroshikh. *Vacuum arc: plasma sources, deposition of coatings, surface modification*. Kiev: "Naukova dumka", 2012.
14. W. Heinke, A. Matthews, G. Berg, C. Friedrich, E. Broszeit. Evaluation of PVD nitride coatings, using impact, scratch and Rockwell-C adhesion tests // *Thin Solid Films*. 1995, v. 270, p. 431-438.
15. G.N. Tolmachova, A.S. Kuprin. Application of the indentation method for investigation of mechanical properties of superhard titanium nitride coatings // *PSE*. 2011, v. 9, N 2, p. 157-163.
16. V.G. Kaplun, N.S. Maijvetj. Research VT8 surface of titanium alloy after nitriding at low temperature plasma discharge glow // *Visnyk dvygunobuduvannya*. 2008, N 2, p. 190-193 (in Ukrainian).
17. K.N. Ramazanov and I.S. Ramazanov. Ion nitriding titanium alloy VT6 glow discharge effect hollow cathode // *Vestnik UGATU (Scientific Journal of Ufa State Aviation Technical University)*. 2014, v. 18, N 2(63), p. 41-46 (in Russian).
18. A.N. Bekrenev and E.A. Filina. Effect of laser alloying on changes in the physical and mechanical properties of the surface layers of titanium // *FHOM (Physics and Chemistry of Materials Processing)*. 1991, N 4, p. 116-121 (in Russian).
19. A. Krella. Cavitation resistance of TiN nanocrystalline coatings with various thickness // *Advances in Materials Science*. 2009, v. 9, N 2(20), p. 12-24.

КАВИТАЦИОННЫЙ ИЗНОС СПЛАВА Ti-6Al-4V С ВАКУУМНО-ДУГОВЫМИ ПОКРЫТИЯМИ TiN И CrN

*А.С. Куприн, В.Д. Овчаренко, С.А. Леонов, Г.Н. Толмачева, В.А. Белоус,
Е.Н. Решетняк, И.О. Клименко, М. Кмеч*

Исследована стойкость к кавитации в дистиллированной воде сплава Ti-6Al-4V с вакуумно-дуговыми покрытиями TiN и CrN. Показано, что покрытия, обладающие высокими механическими свойствами, существенно снижают кавитационный износ сплава, продлевая инкубационный период разрушения и снижая потерю массы. Предварительное ионно-плазменное азотирование сплава приводит к формированию под покрытием твердого переходного слоя, который улучшает адгезию покрытия к сплаву и тем самым увеличивает его стойкость к кавитационному разрушению.

КАВИТАЦІЙНИЙ ЗНОС СПЛАВУ Ti-6Al-4V З ВАКУУМНО-ДУГОВИМИ ПОКРИТТЯМИ TiN ТА CrN

*О.С. Купрін, В.Д. Овчаренко, С.О. Леонов, Г.М. Толмачова, В.А. Білоус,
О.М. Решетняк, І.О. Кліменко, М. Кмеч*

Досліджено стійкість до кавітації в дистильованій воді сплаву Ti-6Al-4V з вакуумно-дуговими покриттями TiN і CrN. Показано, що покриття, які мають високі механічні властивості, істотно знижують кавітаційний знос сплаву, подовжуючи інкубаційний період руйнування і знижуючи втрату маси. Попереднє іонно-плазмове азотування сплаву призводить до формування під покриттям твердого перехідного шару, який покращує адгезію покриття до металу і тим самим збільшує його стійкість до кавітаційного руйнування.